



Published in final edited form as:

Nat Chem. ; 3(8): 615–619. doi:10.1038/nchem.1074.

## A Gateway Synthesis, PKC Affinities and Cell Growth Activities of Daphnane Congeners

Paul A. Wender\*, Nicole Buschmann, Nathan B. Cardin, Lisa R. Jones, Cindy Kan, Jung-Min Kee, John A. Kowalski, and Kate E. Longcore

Departments of Chemistry and Chemical and Systems Biology, Stanford University, Stanford, CA 94305-5080

The daphnane diterpene orthoesters constitute a structurally fascinating family of natural products that exhibit a remarkable range of potent biological activities. While partial activity information is available for some natural daphnanes, little information exists for non-natural congeners or how changes in structure affect mode of action, function, potency or selectivity. A gateway strategy designed to provide general synthetic access to natural and non-natural daphnanes is described and utilized in the synthesis of two novel members of this class. In this study, a commercially available tartrate derivative was elaborated through a key late stage diversification intermediate into B-ring yuanhuapin analogs to initiate exploration of the structure-function relationships of this class. PKC was identified as a cellular target for these agents, and their activity against human lung and leukemia cell lines was evaluated. The natural product and a novel non-natural analog exhibited significant potency while the epimeric epoxide was essentially inactive.

The daphnane diterpene orthoesters (DDOs) constitute a structurally fascinating and synthetically challenging class of natural products, collectively exhibiting a remarkably broad range of biological activities and selectivities.<sup>1–11</sup> Plants containing DDOs have been used medicinally for over 2000 years,<sup>12</sup> and more than 140 unique members have been identified to date. Many DDOs are exceptional, but relatively unexplored, leads for the treatment of cancer, diabetes, neurodegenerative diseases, and neuropathic pain. Some DDOs such as resiniferatoxin (RTX) have advanced into clinical trials.<sup>13–15</sup> Significantly, however, the study of daphnanes has been hampered by their scarce supply and high cost (generally >\$50/mg), often exacerbated by geopolitical issues in accessing sources, and further limited by their synthetic inaccessibility and the paucity of methods for their selective modification. RTX is the only DDO to be synthesized to date,<sup>16</sup> however, it lacks

Users may view, print, copy, download and text and data-mine the content in such documents, for the purposes of academic research, subject always to the full Conditions of use: [http://www.nature.com/authors/editorial\\_policies/license.html#terms](http://www.nature.com/authors/editorial_policies/license.html#terms)

wenderp@stanford.edu.

### Author contributions

P.A.W., N.B., N.B.C., L.R.J., C.K., J.M.K., J.A.K., and K.E.L. conceived and designed the experiments. N.B., N.B.C., L.R.J., C.K., J.M.K., J.A.K., and K.E.L. performed the experiments. N.B., N.B.C., L.R.J., C.K., J.M.K., J.A.K., and K.E.L. analyzed the data. P.A.W., N.B.C., and K.E.L. co-wrote the paper. All authors commented on the manuscript.

The authors declare no competing financial interests.

Supplementary information and chemical compound information accompany this paper at [www.nature.com/naturechemistry](http://www.nature.com/naturechemistry). Reprints and permission information is available online at <http://npg.nature.com/reprintsandpermissions/>. Correspondence and requests for materials should be addressed to P.A.W.

key functionalities (e.g., C5, C12 and C18 oxygenation) needed to fully investigate the therapeutic potential of the DDOs. More significantly and a major point of increasing emphasis is that these natural products are neither evolved nor optimized for human use. Thus while they represent promising leads, little if any information exists on the activity of structural analogs needed to design less complex and potentially therapeutically superior agents. We disclose herein a “gateway strategy” that is designed to address two interconnected goals: (1) to develop a synthetic route to enable general access to DDOs and more importantly their as yet unexplored analogs from a common differentially protected precursor and (2) to exploit this capability to investigate the structural basis for their activities and their therapeutic potential. As in our other function oriented synthesis programs (e.g., phorbol, bryostatin, prostratin),<sup>17–18</sup> these studies are expected to inform the design and synthesis of structurally simpler targets with activities comparable to or better than the natural products.

A major subset of DDOs, depicted in Figure 1, is made up of at least 73 congeners differing in the functionality at C12, the orthoester sidechain, A-ring oxidation, and the substitution at C20. This subfamily includes yuanhuapin (**1**), which was first isolated in 1986 from the flowers of *Daphne genkwa*,<sup>19</sup> one of the 50 fundamental herbs in Chinese traditional medicine. In addition to possessing anticancer activity,<sup>20</sup> yuanhuapin also displays structural features shared by many biologically active DDOs. Significantly, several of these DDOs display over 1000-fold greater activity against A549 human lung cancer cells relative to MRC-5 normal lung epithelial cells.<sup>5</sup> By initially targeting yuanhuapin analogs, we sought to begin to identify the structural requirements for the activities of these and related daphnane leads, their biological targets, and their modes of action. This study would thus complement and supplement the natural DDO library by addressing structural issues that cannot be investigated with the known natural products. As evident from studies on taxotere, halichondrin, and our own bryostatin, prostratin, and octaarginine drug delivery programs,<sup>17</sup> such information can be used to design simpler and more effective clinical leads. A first issue of importance in this inaugural DDO study was to investigate the role of the B-ring epoxide common to the majority of members of the DDO family.

Our retrosynthetic analysis (Figure 1) focused on the DDO class rather than on a single synthetic target with the goal of ultimately establishing a systematically varied library of natural and non-natural members. Step economy arises in this strategy through the development of a single synthetic route to an advanced intermediate that upon late-stage differential diversification would provide access to the greatest number of targets in short parallel sequences. The highly oxygenated intermediate **5** serves this gateway function, allowing for differential modification of key conserved functionalities (orthoester, oxygens at C3, C4, C5 and C20) and retention or deletion of oxygens at other sites. Importantly, the gateway structure **5** would enable access to a majority of daphnanes and their as yet unexplored analogs. Access to **5** was expected to draw on a palladium-catalyzed cyclization of **7**, whose allyl and alkynyl appendages would be stereoselectively introduced by exploiting the conformationally fixed and facially biased oxabicyclic core of **8**. This BC-core would be convergently assembled from commercially available kojic acid and a tartrate-derived bromide via a novel Claisen rearrangement of **9** followed by a

diastereoselective oxidopyrylium [5 + 2] cycloaddition. The absolute stereochemistry of **9** would ultimately derive from the D-dimethyltartrate derivative **11**.

## Results

Our synthesis began with conversion of **11** to the corresponding  $C_2$ -symmetric diol **12**<sup>21</sup> (Figure 2). Subsequent desymmetrization through monobenzyl ether formation afforded secondary allylic alcohol **13**, from which the primary allylic bromide **14** was readily obtained. This fragment containing eight carbons of the target was then convergently joined to the six-carbon fragment of kojic acid by alkylation of potassium kojate. Upon heating neat, the *O*-linked product **9** was converted, after bis-silyl ether formation, to the *C*-linked Claisen product **15** in good isolated yield and with excellent diastereoselectivity. This is a relatively underexplored type of Claisen rearrangement in which stereoinduction is controlled by a stereocenter external to rather than within the six-centered transition state. We propose that the preferred transition state of the Claisen rearrangement reported herein can be explained with the “inside alkoxy” effect, which has been described for Diels-Alder and 1,3-dipolar cycloadditions.<sup>22</sup> Heating the Claisen product **15** (microwave) effected silyl migration to form the oxidopyrylium intermediate,<sup>23–27</sup> which underwent cycloaddition to give the bicyclic BC-core **8**. Conventional heating also provided the desired product; however, extended reaction times were required. Additionally, a one-flask procedure to effect the Claisen rearrangement/oxidopyrylium [5 + 2] cycloaddition was developed; although, the two-flask procedure was adopted for material throughput considerations (see Supplementary Information for details). Due to the conformational preferences of the tether substituents, only one diastereomer of the BC-core was expected and observed.<sup>28</sup> Significantly, only six linear steps are required to produce **8** from commercially available starting materials.

With the ether bridged oxidopyrylium cycloadduct **8** conformationally constrained and facially biased, the approach of incoming reagents in subsequent steps was expected to and indeed did occur exclusively from the  $\alpha$ -face. Thus,  $\alpha$ -allyl addition to the C10 ketone in **8** gave the C10  $\beta$ -alcohol, which upon treatment with thionyl bromide underwent syn 1,3-transposition to the C5 $\beta$ -bromide **16**. Treatment of this silylenol ether with tetrabutylammonium fluoride (TBAF) resulted in exclusive  $\alpha$ -protonation at C10 to provide the corresponding crystalline bromoketone (X-ray, see Supplementary Information). Addition of phenylacetylide to this ketone proceeded in excellent yield and with  $\alpha$ -face selectivity to provide the tricyclic core precursor **7**. Subsequent palladium-catalyzed cyclization<sup>29</sup> was best achieved with formic acid<sup>30</sup> and polymethylhydrosiloxane (PMHS) to reveal the complete daphnane tricyclic core (**6**) in only 11 steps from tartrate. Rhodium-catalyzed cyclization<sup>31</sup> provided the tricyclic core with the opposite selectivity for the C2-methyl epimer (see Supplementary Information for details). The step economical route to the complete ABC daphnane-tricycle **6** represents a significant advancement relative to the 20 synthetic operations employed to access an analogous intermediate in the synthesis of RTX.<sup>16</sup> Significantly, **6** is also more highly oxidized (C5, C12, and C18) than the corresponding RTX intermediate, which is vital for subsequent functionalization towards the broader family of DDOs and functional analogs.

Global ozonolysis of tricyclic core **6** then afforded the corresponding crystalline ketoaldehyde (X-ray, see Supplementary Information), which was reduced using Luche conditions. Zinc-mediated reductive fragmentation of the bridging ether was followed by vanadium-catalyzed epoxidation of the C5,C6 alkene, which proceeded with concomitant opening of the epoxide by the C9 alcohol to provide overall substitution of the C5 bromide by oxygen with retention of C5 stereochemistry. A number of allylic oxidations were attempted to install the desired oxygenation without reformation of the bridging ether; however, it was found that this functionality provided facial selectivity during installation of the isopropenyl unit (vide infra). Differential protection of the oxygens in **17** provided **18**, which upon oxidation at C13 and treatment of the resulting ketone with isopropenyl lithium in the presence of cerium trichloride gave the desired  $\beta$ -adduct **5** in 49% over two steps. This gateway intermediate, available in 21 steps, incorporates the complete daphnane skeleton with a fully differentiated and rich array of functionality.

While a C11 oxymethyl substituent is found in some daphnanes and will be exploited in future diversification studies, this inaugural study focused on accessing C11 methyl targets. Accordingly, polycycle **5** was converted to pentaol **19** whose primary hydroxyl groups were simultaneously replaced with iodides (Figure 3). The cyclic carbonate (step d) was essential, and failure to protect the C13-alcohol resulted in C13,C18-ether formation during triflation. Subsequent zinc-mediated reduction differentially converted the C11 iodomethyl to the desired methyl group and cleaved the bridging B-ring ether to afford exo alkene **20**. Introduction of the B-ring allylic acetate to the C4,C5-acetonide intermediate derived from **20** was initiated by allylic bromination, which chemoselectively converted the exo alkene with transposition to an allylic bromide without interference from the carbonate-deactivated isopropenyl group. The resultant primary allylic bromide was then displaced with acetate to give alkene **21**. Removal of both the acetate and carbonate groups was followed by esterification of the C14 and C20 alcohols, which served to protect the C20 alcohol while setting the stage for another key challenge, C14-ester initiated orthoester formation. Gratifyingly, heating bis-benzoate **22** to 200 °C (microwave) in the presence of *p*-TsOH produced the orthoester, and subsequent acetylation provided **23** in 44% yield (two steps). Removal of the C3 silyl ether using TAS-F<sup>32</sup> (use of TBAF lead to significant cleavage of the primary benzoate) was followed by oxidation of the resulting alcohol to the ketone,<sup>33</sup> thus completing the A-ring. Methanolysis of the C20 benzoate followed by hydrolysis of the acetonide<sup>34</sup> provided des-epoxy-yuanhuapin (**3**). Model studies of the epoxidation using phorbol-12,13-dibutyrate demonstrated that a reagent controlled epoxidation<sup>35</sup> can overcome the inherent facial bias of the seven-membered B-ring of this substrate<sup>36</sup> and deliver principally the  $\alpha$ -epoxide. However, because direct epoxidation of **3** provided the  $\beta$ -epoxide of yuanhuapin (**2**), optimization of this process was deferred to conserve material for critical assays and because a small sample of authentic yuanhuapin was in hand for assay comparisons. Evidence suggests that the C5-alcohol and/or the oxidation of the A-ring play important roles in determining the stereochemical outcome of the epoxidation of des-epoxy-yuanhuapin.

The synthetic availability of **2** and **3** made possible for the first time the start of a comparative analysis of factors that contribute to daphnane activity, including the

unexplored role of the ubiquitous C6,C7- $\alpha$ -epoxide, and identification of their biological targets. While yuanhuapin was originally reported to be a DNA topoisomerase I inhibitor,<sup>37</sup> several DDOs are known to activate protein kinase C (PKC), a family of serine/threonine kinases involved in myriad biological processes through its role in signal transduction. We therefore tested the systematically varied triad **1–3** in a cell-free PKC binding assay. Significantly, we found that yuanhuapin is a highly potent (*subnanomolar*) ligand for PKC (Table 1), a target that has implications for treating diseases including cancer,<sup>38</sup> Alzheimer's,<sup>39</sup> and HIV/AIDS.<sup>40–41</sup> It is especially noteworthy that **3** exhibits single digit nanomolar affinity to PKC. In striking contrast, C6,C7-*epi*-yuanhuapin (**2**) displays nearly three orders of magnitude lower affinity than the  $\alpha$ -epoxide. Additionally, the potency trends observed in this cell-free assay for the three compounds were mirrored in cellular assays (Table 1). Yuanhuapin (**1**) was reported to have growth inhibition activity in A549 cells (human lung carcinoma);<sup>20</sup> therefore, evaluation of the triad of targets in this cell line was conducted. In addition, all three orthoester-containing compounds were assayed for activity in K562 (human chronic myelogenous leukemia) cells based on the reported activities of three naturally occurring DDOs in this cell line (gnidimacrin, huratoxin, and mezerein have been screened by the Developmental Therapeutics Program NCI/NIH in this cell line). Significantly, des-epoxy-yuanhuapin (**3**) and yuanhuapin (**1**) inhibited cell proliferation in both cell lines, while the unnatural  $\beta$ -epoxide (**2**) was essentially inactive. Consistent with the role of PKC in these cellular assays, co-administration of **1** or **3** with Gö6983,<sup>42</sup> a broad spectrum PKC inhibitor, abrogated growth inhibition in both A549 and K562 cells.

## Discussion

A gateway strategy was developed to access daphnane inspired targets, which in turn led to the identification of a cellular mediator of their activity. For this inaugural study, the previously unexplored yuanhuapin analogs **2** and **3** were selected for evaluation as they make possible comparative systematic analysis of the role of a commonly encountered B-ring epoxide in DDO activity, including whether the epoxide is required or could be replaced with a less complex and more stable alkene. The synthesis employed a novel Claisen rearrangement to transfer tartrate derived chirality to a pro-C11 center, which in turn controlled stereoselectivity in one of the most complex [5+2] oxidopyrylium cycloadditions studied to date. The facial bias of the resulting oxygen bridged B-ring cycloadduct was then used to control introduction of C10 and C4 stereochemistry. Further elaboration, including construction of the A-ring and completion of the carbon skeleton, provided **5**. This advanced intermediate can be used as a starting point for step economical access to a range of targets required for understanding the structural basis for daphnane activity, which in turn would allow for the design of simpler but potentially more active agents. Congeners **1–3** were identified as ligands for PKC with **1** and **3** exhibiting subnanomolar and single digit nanomolar affinities, respectively, a new finding that tracks with cell growth inhibition activity and is pertinent to ongoing synthetic and mode of action studies. Furthermore, identification of the profound effect that B-ring functionality has in determining PKC binding affinities across this series is consistent with a model in which oxygens present along the southern edge make contact with PKC.<sup>43–44</sup> Installation of the  $\beta$ -epoxide, as in **2**,

significantly perturbs the location of the hydroxymethyl relative to **1**, whereas replacement of the epoxide with an alkene, as in **3**, preserves the spatial arrangement of oxygens present in the natural product (global minimum conformations of **1–3** were determined with MM3\* Monte Carlo conformation searches). This finding demonstrates how the gateway strategy disclosed herein enables elucidation of the structural requirements of DDOs for PKC activation and begins a systematic approach to simplified and improved agents.

## Methods

Full experimental details for the synthesis of all new compounds including procedures, spectral data, and characterization can be found in the Supplemental Information. Protocols for the cell-free competitive binding assay and growth inhibition experiments can also be found in the Supplemental Information.

## Supplementary Material

Refer to Web version on PubMed Central for supplementary material.

## Acknowledgments

This research was supported by the National Institutes of Health (CA31841). Additional funding was provided by the Alexander von Humboldt Foundation (N.B.), Stanford Graduate Fellowships from the Office of the Vice Provost for Graduate Education (N.B.C.) and the Office of Technology Licensing (K.E.L.), Bristol-Myers Squibb Graduate Fellowship in Organic Chemistry (J.A.K.), Amgen Graduate Fellowship (C.K.), and Eli Lilly Graduate Research Fellowships (N.B.C., J.A.K., J.M.K.). J.-M. Yue is thanked for kindly supplying a sample of yuanhuapin for biological evaluation. L. Cegelski is acknowledged for graciously providing access to tissue culture space and equipment. K. Cimprich generously contributed A549 and K562 cells. X-ray crystallography was performed at the University of California, Berkeley and analyzed by X. Ottenwaelder or collected and analyzed by A. Oliver.

## References

1. Liao SG, Chen HD, Yue JM. Plant orthoesters. *Chem Rev.* 2009; 109:1092–1140. [PubMed: 19182998]
2. Miyamae Y, Villareal MO, Abdrabbah MB, Isoda H, Shigemori H. Hirseins A and B, daphnane diterpenoids from *Thymelaea hirsuta* that inhibit melanogenesis in B16 melanoma cells. *J Nat Prod.* 2009; 72:938–941. [PubMed: 19284745]
3. Chen H-D, He X-F, Ai J, Geng M-Y, Yue J-M. Trigochilides A and B, two highly modified daphnane-type diterpenoids from *Trigonostemon chinensis*. *Org Lett.* 2009; 11:4080–4083. [PubMed: 19702252]
4. Hayes PY, Chow S, Somerville MJ, De Voss JJ, Fletcher MT. Pimelotides A and B, diterpenoid ketal-lactone orthoesters with an unprecedented skeleton from *Pimelea elongata*. *J Nat Prod.* 2009; 72:2081–2083. [PubMed: 19968293]
5. Hong J-Y, Nam J-W, Seo E-K, Lee SK. Daphnane diterpene esters with anti-proliferative activities against human lung cancer cells from *Daphne genkwa*. *Chem Pharm Bull.* 2010; 58:234–237. [PubMed: 20118586]
6. Zhang L, et al. Highly functionalized daphnane diterpenoids from *Trigonostemon thyrsoides*. *Org Lett.* 2010; 12:152–155. (ref. 7 suggests revision of the DDOs disclosed in this publication). [PubMed: 19968236]
7. Chen H-D, et al. Trigochinins A-C: Three new daphnane-type diterpenes from *Trigonostemon chinensis*. *Org Lett.* 2010; 12:1168–1171. [PubMed: 20148570]
8. Chen H-D, et al. Trigochinins D-I: Six new daphnane-type diterpenoids from *Trigonostemon chinensis*. *Tetrahedron.* 2010; 66:5065–5070.

9. Lin B-D, et al. Trigoxypins A-G: Diterpenes from *Trigonostemon xyphophylloides*. *J Nat Prod.* 2010; 73:1301. [PubMed: 20593838]
10. Li LZ, Gao PY, Peng Y, Wang LH, Song SJ. A novel daphnane-type diterpene from the flower bud of *Daphne genkwa*. *Chem Nat Compd.* 2010; 46:380–382.
11. Li L-Z, et al. Daphnane-type diterpenoids from the flower buds of *Daphne genkwa*. *Helv Chim Acta.* 2010; 93:1172–1179.
12. Appendino G, Szallasi A. Euphorbium: Modern research on its active principle, resiniferatoxin, revives an ancient medicine. *Life Sciences.* 1997; 60:681–696. [PubMed: 9064473]
13. Mourtzoukou EG, Iavazzo C, Falagas MF. Resiniferatoxin in the treatment of interstitial cystitis: A systematic review. *Int Urogynecol J.* 2008; 19:1571–1576.
14. MacDonald R, Monga M, Fink HA, Wilt TJ. Neurotoxin treatments for urinary incontinence in subjects with spinal cord injury or multiple sclerosis: A systematic review of effectiveness and adverse effects. *J Spinal Cord Med.* 2008; 31:157–165. [PubMed: 18581662]
15. Wong GY, Gavva NR. Therapeutic potential of vanilloid receptor TRPV1 agonists and antagonists as analgesics: Recent advances and setbacks. *Brain Res Rev.* 2009; 60:267–277. [PubMed: 19150372]
16. Wender PA, et al. The first synthesis of a daphnane diterpene: The enantiocontrolled total synthesis of (+)-resiniferatoxin. *J Am Chem Soc.* 1997; 119:12976–12977.
17. Wender PA, Verma VA, Paxton TJ, Pillow TH. Function-oriented synthesis, step economy, and drug design. *Acc Chem Res.* 2008; 41:40–49. [PubMed: 18159936]
18. Wender PA, Miller BL. Synthesis at the molecular frontier. *Nature.* 2009; 460:197–201. [PubMed: 19587760]
19. Hu B-H, Huai S, He Z-W, Wu X-C. Studies on the constituent of the yuanyuan's flower buds. *Acta Chim Sinica.* 1986; 44:843–845.
20. Zhan Z-J, Fan C-Q, Ding J, Yue J-M. Novel diterpenoids with potent inhibitory activity against endothelium cell HMEC and cytotoxic activities from a well-known TCM plant *Daphne genkwa*. *Bioorg Med Chem.* 2005; 13:645–655. [PubMed: 15653331]
21. Jørgensen N, Iversen EH, Paulsen AL, Madsen R. Efficient synthesis of enantiopure conduritols by ring-closing metathesis. *J Org Chem.* 2001; 66:4630–4634. [PubMed: 11421784]
22. Houk KN, et al. Stereoselective nitrile oxide cycloadditions to chiral allyl ethers and alcohols. The “inside alkoxy” effect. *J Am Chem Soc.* 1984; 106:3880–3882.
23. Wender PA, McDonald FE. Studies on tumor promoters 9. A second-generation synthesis of phorbol. *J Am Chem Soc.* 1990; 112:4956–4958.
24. Wender PA, Mascareñas JL. Studies on tumor promoters 11. A new [5 + 2] cycloaddition method and its application to the synthesis of BC ring precursors of phorboids. *J Org Chem.* 1991; 56:6267–6269.
25. Domingo LR, Zaragoza RJ. Toward an understanding of the mechanisms of the intramolecular [5 + 2] cycloaddition reaction of  $\gamma$ -pyrones bearing tethered alkenes. A theoretical study. *J Org Chem.* 2000; 65:5480–5486. [PubMed: 10970285]
26. Zaragoza RJ, Aurell MJ, Domingo LR. The role of the transfer group in the intramolecular [5 + 2] cycloadditions of substituted  $\beta$ -hydroxy- $\gamma$ -pyrones: A DFT analysis. *J Phys Org Chem.* 2005; 18:610–615.
27. Singh V, Krishna UM, Vikrant, Trivedi GK. Cycloaddition of oxidopyrylium species in organic synthesis. *Tetrahedron.* 2008; 64:3405–3428.
28. Wender PA, et al. Studies on oxidopyrylium [5 + 2] cycloadditions: Toward a general synthetic route to the C12-hydroxy daphnetoxins. *Org Lett.* 2006; 8:5373–5376. [PubMed: 17078721]
29. Trost BM, Rise F. A reductive cyclization of 1,6- and 1,7-enynes. *J Am Chem Soc.* 1987; 109:3161–3163.
30. Trost BM, Li Y. A new catalyst of Pd catalyzed Alder ene reaction. A total synthesis of (+)-cassiol. *J Am Chem Soc.* 1996; 118:6625–6633.
31. Jang HY, Krische MJ. Rhodium-catalyzed reductive cyclization of 1,6-diyne and 1,6-enynes mediated by hydrogen: Catalytic C-C bond formation via capture of hydrogenation intermediates. *J Am Chem Soc.* 2004; 126:7875–7880. [PubMed: 15212535]

32. Scheidt KA, et al. Tris(dimethylamino)sulfonium difluorotrimethylsilicate, a mild reagent for the removal of silicon protecting groups. *J Org Chem.* 1998; 63:6436–6437.
33. Nicolaou KC, Zhong Y-L, Baran PS. A new method for the one-step synthesis of  $\alpha,\beta$ -unsaturated carbonyl compounds from saturated alcohols and carbonyl compounds. *J Am Chem Soc.* 2000; 122:7596–7597.
34. Lipshutz BH, Harvey DF. Hydrolysis of acetals and ketals using  $\text{LiBF}_4$ . *Synth Commun.* 1982; 12:267–277.
35. Zhang W, Basak A, Kosugi Y, Hoshino Y, Yamamoto H. Enantioselective epoxidation of allylic alcohols by a chiral complex of vanadium: An effective controller system and a rational mechanistic model. *Angew Chem Int Ed.* 2005; 44:4389–4391.
36. Schmidt R, Hecker E. Autoxidation of phorbol esters under normal storage conditions. *Cancer Res.* 1975; 35:1375–1377. [PubMed: 1120318]
37. Zhang S, et al. Preparation of yuanhuacine and relative daphne diterpene esters from *Daphne genkwa* and structure-activity relationship of potent inhibitory activity against DNA topoisomerase I. *Bioorg Med Chem.* 2006; 14:3888–3895. [PubMed: 16488610]
38. Griner EM, Kazanietz MG. Protein kinase C and other diacylglycerol effectors in cancer. *Nat Rev Cancer.* 2007; 7:281–294. [PubMed: 17384583]
39. Alkon DL, Sun M-K, Nelson TJ. PKC signaling deficits: A mechanistic hypothesis for the origins of Alzheimer's disease. *Trends Pharmacol Sci.* 2007; 28:51–60. [PubMed: 17218018]
40. Richman DD, et al. The challenge of finding a cure for HIV infection. *Science.* 2009; 323:1304–1307. [PubMed: 19265012]
41. Wender PA, Kee J-M, Warrington JM. Practical synthesis of prostratin, DPP, and their analogs, adjuvant leads against latent HIV. *Science.* 2008; 320:649–652. [PubMed: 18451298]
42. Toullec D, et al. The bisindolylmaleimide GF 109203X is a potent and selective inhibitor of protein kinase C. *J Biol Chem.* 1991; 266:15771–15781. [PubMed: 1874734]
43. Zhang G, Kazanietz MG, Blumberg PM, Hurley JH. Crystal structure of the Cys2 activator-binding domain of protein kinase C $\delta$  in complex with phorbol ester. *Cell.* 1995; 81:917–924. [PubMed: 7781068]
44. Koehler KF, Sharkey NA, Dell'Aquila ML, Blumberg PM. Analysis of the phorbol ester pharmacophore on protein kinase C as a guide to the rational design of new classes of analogs. *Proc Natl Acad Sci USA.* 1986; 83:4214–4218. [PubMed: 3086877]

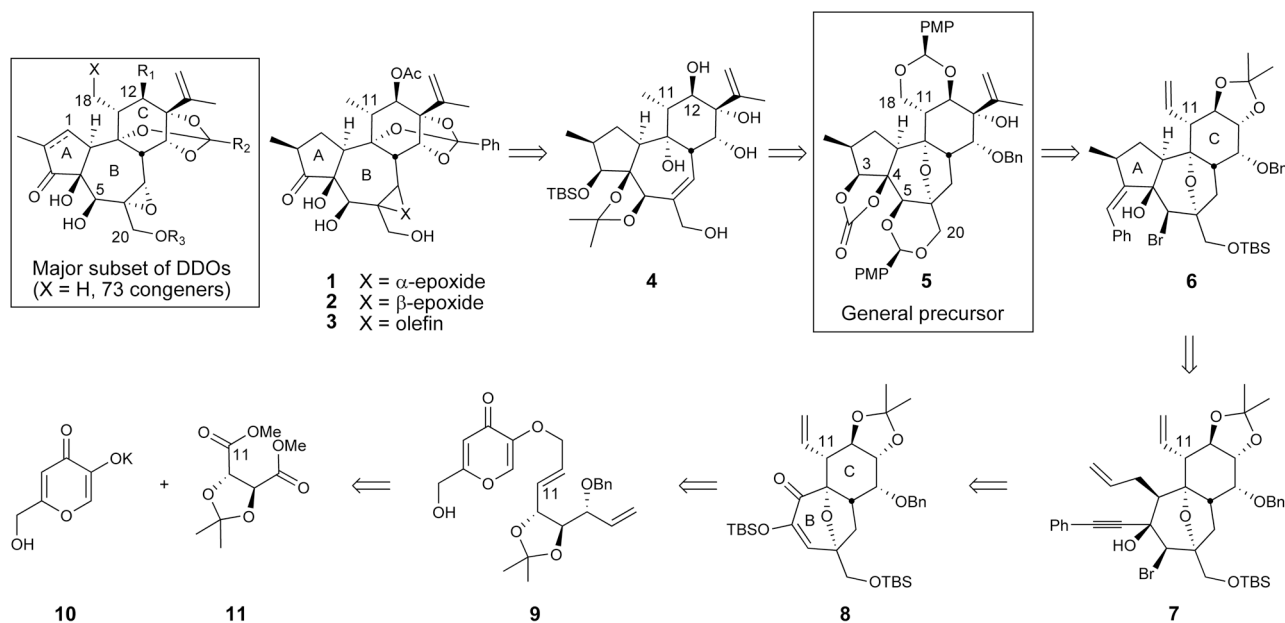


**Figure 1. Retrosynthetic analysis for a major subset of natural and non-natural DDOs**

Introduction of the orthoester and functionalization of C3, C12, C18, and C20 from the general precursor **5** was designed to allow divergent access to a broad family of natural and non-natural DDOs. Assembly of the A-ring of this general precursor was envisioned to arise from cyclization of appropriately functionalized enyne **7**. An intramolecular oxidopyrylium cycloaddition was planned to provide the BC-core from alkylated kojic acid derivative **9**, which would be accessed from the readily available potassium salt of kojic acid (**10**) and tartrate derivative **11**.

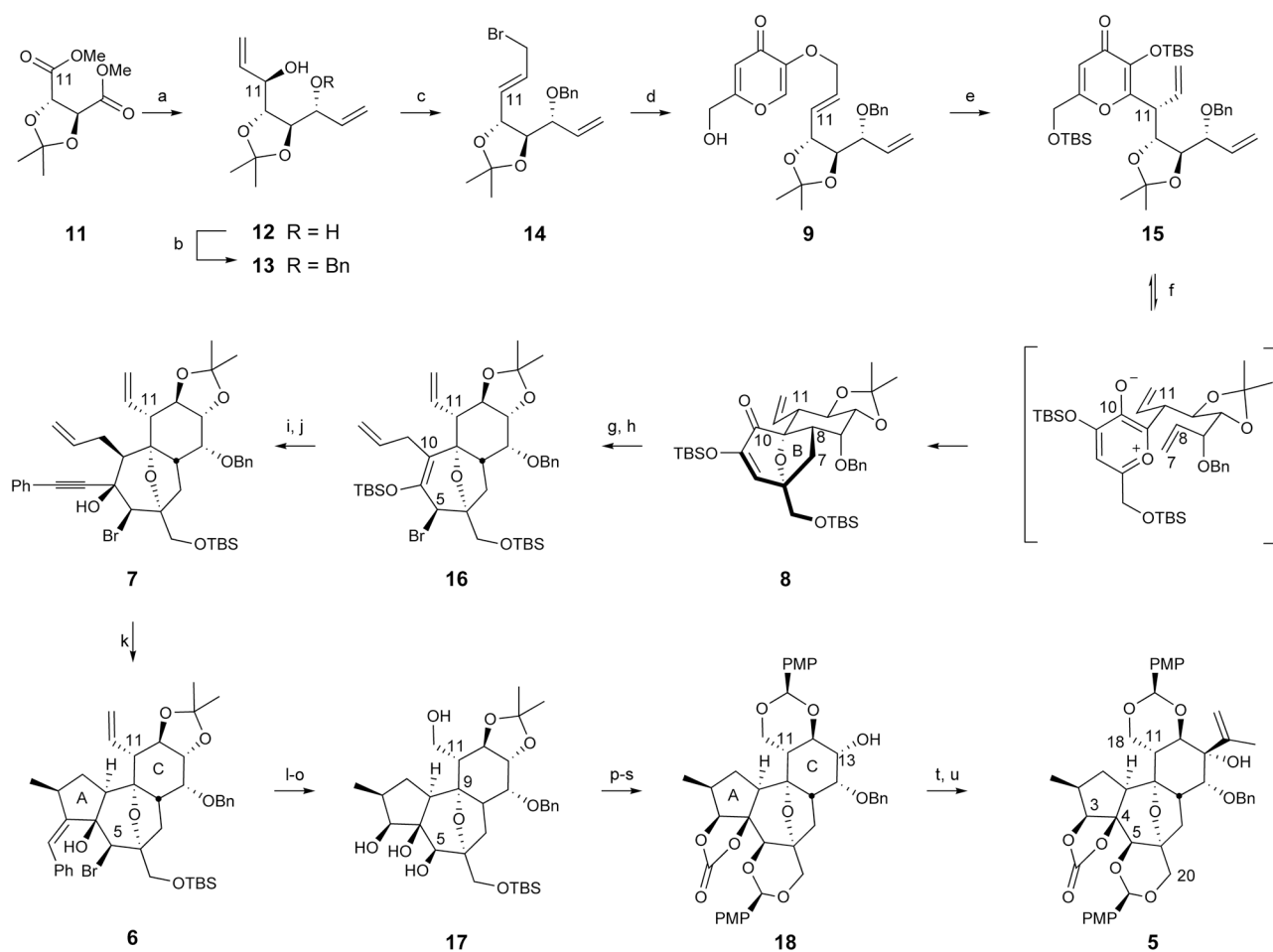


**Figure 2. Synthesis of the complete daphnane skeleton (5)**

Conditions: (a) DIBAL, toluene,  $-78\text{ }^{\circ}\text{C}$ , then divinylzinc,  $-78\text{ }^{\circ}\text{C}$  to r.t. (6:1 ratio of diastereomers), 80%; (b) NaH, BnBr, DMF,  $0\text{ }^{\circ}\text{C}$  to r.t., 86%; (c)  $\text{PPh}_3$ ,  $\text{CBr}_4$ ,  $\text{CH}_2\text{Cl}_2$ ,  $0\text{ }^{\circ}\text{C}$  to r.t., 86%; (d) **10**, *i*-PrOH,  $80\text{ }^{\circ}\text{C}$ , 78%; (e) neat,  $122\text{ }^{\circ}\text{C}$ , then TBS-Cl, imidazole,  $\text{CH}_2\text{Cl}_2$ , r.t. (10:1 ratio of diastereomers), 74%; (f) 1,2-dichlorobenzene,  $250\text{ }^{\circ}\text{C}$ , microwave, 91%; (g) Mg,  $\text{I}_2$ , allyl bromide,  $\text{Et}_2\text{O}$ ,  $0\text{ }^{\circ}\text{C}$ , 93%; (h)  $\text{SOBr}_2$ , pyridine,  $\text{Et}_2\text{O}$ ,  $-40\text{ }^{\circ}\text{C}$ , 82%; (i) TBAF, AcOH, THF,  $0\text{ }^{\circ}\text{C}$ , 84%; (j)  $\text{PhCCH}$ ,  $\text{MeLi} \cdot \text{LiBr}$ , THF,  $-78\text{ }^{\circ}\text{C}$  to r.t., 92%; (k)  $\text{Pd}_2(\text{dba})_3 \cdot \text{CHCl}_3$  (1 mol %), PMHS (10 eq),  $\text{HCOOH}$  (3 eq),  $\text{PhCH}_3$ , r.t., 80%; (l)  $\text{O}_3$ ,  $\text{CH}_2\text{Cl}_2/\text{MeOH}$ ,  $-78\text{ }^{\circ}\text{C}$ , then thiourea, 89%; (m)  $\text{NaBH}_4$ ,  $\text{CeCl}_3 \cdot 7\text{H}_2\text{O}$ ,  $\text{CH}_2\text{Cl}_2/\text{MeOH}$ ,  $-78\text{ }^{\circ}\text{C}$  to r.t., 79%; (n) Zn,  $\text{NH}_4\text{Cl}$ , EtOH,  $55\text{ }^{\circ}\text{C}$ , 89%; (o)  $\text{VO}(\text{acac})_2$ , *t*-BuOOH,  $\text{CH}_2\text{Cl}_2$ , r.t., 84%; (p) TBS-Cl, imidazole,  $\text{CH}_2\text{Cl}_2$ , r.t.; (q) triphosgene, pyridine,  $\text{CH}_2\text{Cl}_2$ , r.t., 86% (two steps); (r) TBAF, THF,  $0\text{ }^{\circ}\text{C}$  to r.t.; (s)  $(\text{PMP})\text{CH}(\text{OMe})_2$ , *p*-TsOH,  $\text{CH}_2\text{Cl}_2$ , r.t., 93% (two steps); (t) Dess-Martin periodinane,  $\text{NaHCO}_3$ ,  $\text{CH}_2\text{Cl}_2$ , r.t.; (u) isopropenyl lithium,  $\text{CeCl}_3$ , THF,  $-78\text{ }^{\circ}\text{C}$ , 49% (two steps).

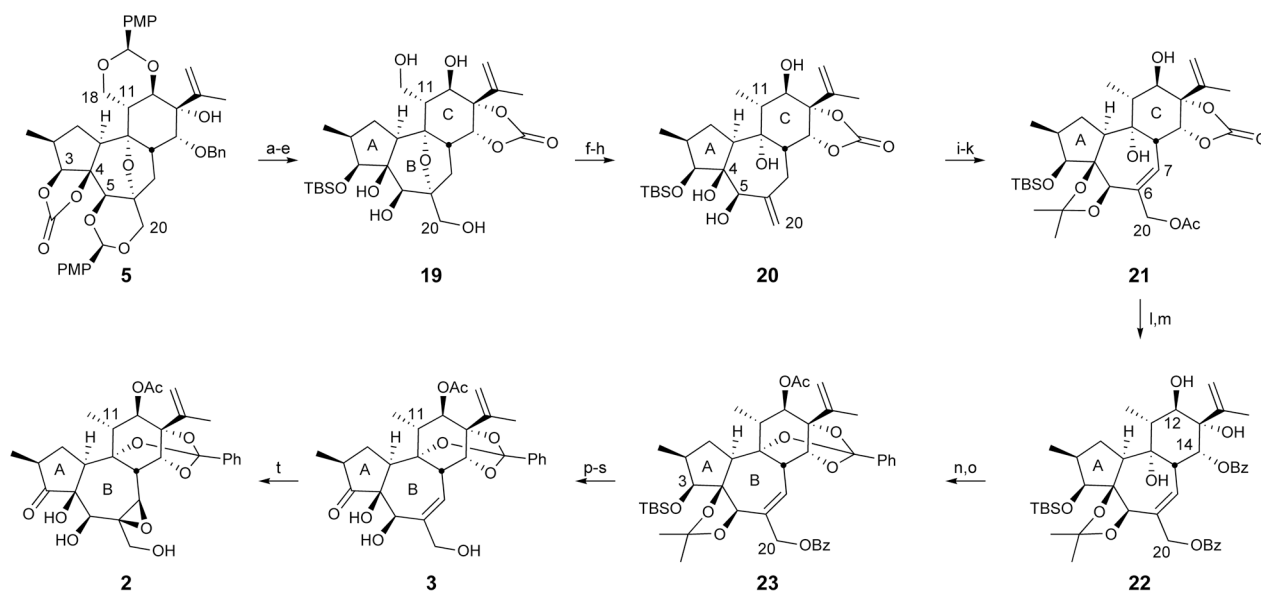


**Figure 3. Completion of des-epoxy- and C6,C7-epi-yuanhuapin**

Conditions: (a)  $K_2CO_3$ , MeOH/H<sub>2</sub>O, 50 °C, 76%; (b) TBS-OTf, 2,6-lutidine, CH<sub>2</sub>Cl<sub>2</sub>, 0 °C, 97%; (c) Li-naphthalenide, THF, -30 °C, 88%; (d) triphosgene, pyridine, CH<sub>2</sub>Cl<sub>2</sub>, r.t., 94%; (e) 4:1:1 AcOH:THF:H<sub>2</sub>O, r.t., 82%; (f) Tf<sub>2</sub>O, 2,6-lutidine, CH<sub>2</sub>Cl<sub>2</sub>, -78 °C; (g) TBAI, CH<sub>3</sub>CN, 65 °C, 93% (two steps); (h) Zn, NH<sub>4</sub>Cl, EtOH, 160 °C, microwave, 77%; (i) 2,2-dimethoxypropane, PPTS, CH<sub>2</sub>Cl<sub>2</sub>, 40 °C, 86%; (j) NBS, (BzO)<sub>2</sub>, NaHCO<sub>3</sub>, CCl<sub>4</sub>/PhH, 70 °C; (k) KOAc, 18-crown-6, CH<sub>3</sub>CN, r.t., 52% (two steps, 39% RSM); (l) LAH, THF, 0 °C to r.t., 75%; (m) BzCl, DMAP, Et<sub>3</sub>N, CH<sub>2</sub>Cl<sub>2</sub>, r.t., 90%; (n) *p*-TsOH, MeOH, DMF, 200 °C, microwave, 49% (11% RSM); (o) Ac<sub>2</sub>O, DMAP, CH<sub>2</sub>Cl<sub>2</sub>, r.t., 90%; (p) TAS-F, DMF, r.t., 89%; (q) IBX, DMSO/PhCH<sub>3</sub>, 70 °C, 97%; (r)  $K_2CO_3$ , MeOH, r.t.; (s) LiBF<sub>4</sub>, H<sub>2</sub>O/CH<sub>3</sub>CN, 70 °C, 29% (two steps); (t) VO(O<sup>*i*</sup>Pr)<sub>3</sub>, *t*-BuOOH, (1*S*,2*S*)-*N,N'*-dihydroxy-*N,N'*-bis(3,3,3-triphenylpropionyl)-1,2-cyclohexanediamine, CH<sub>2</sub>Cl<sub>2</sub>/PhH, 4 °C, 81%.

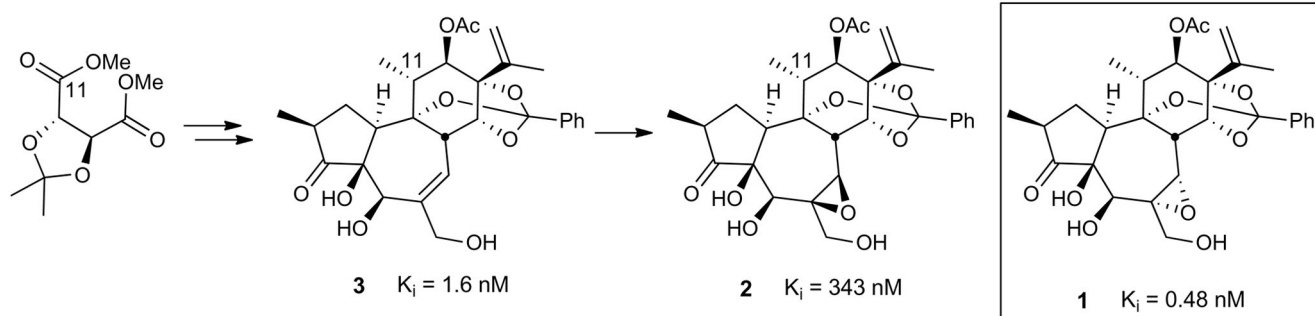


Figure 4.

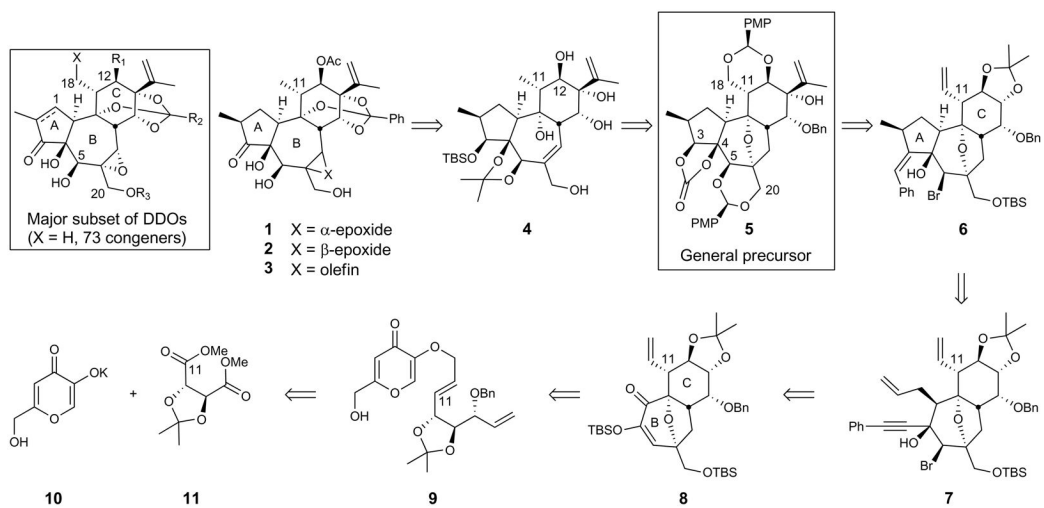


Figure 5.

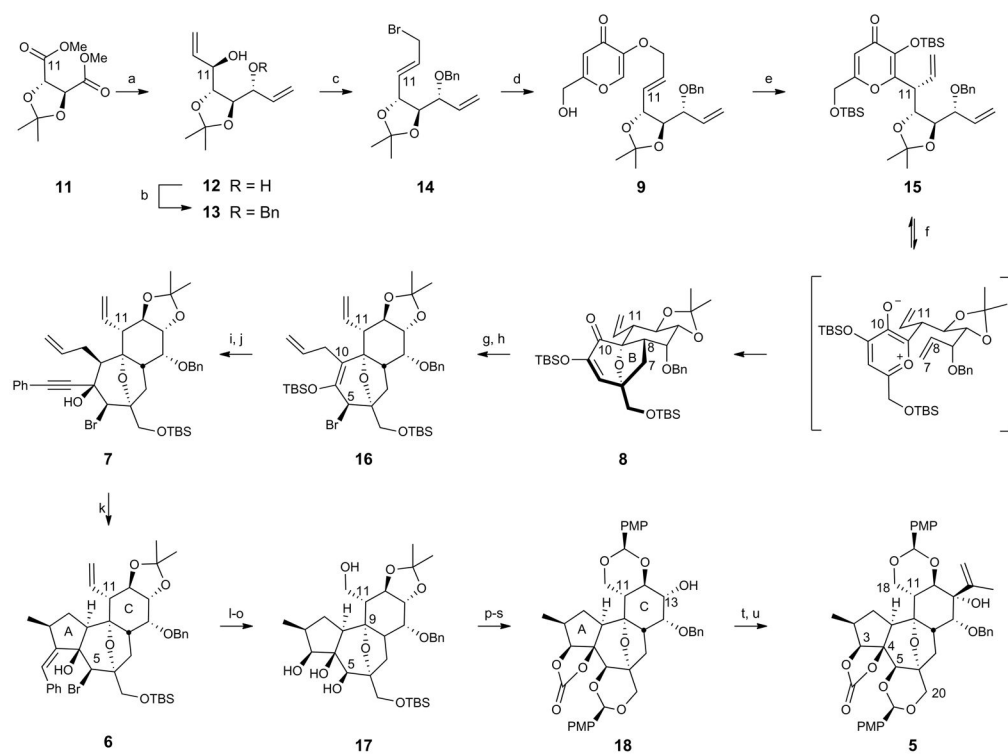
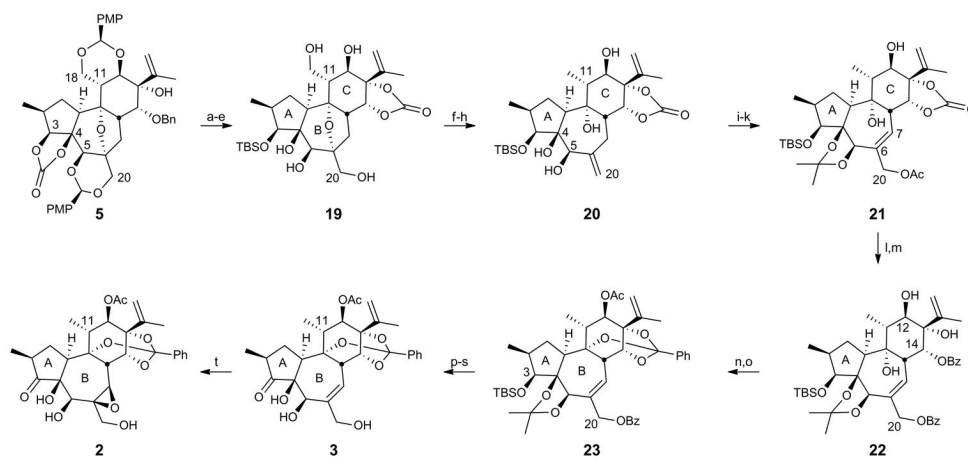
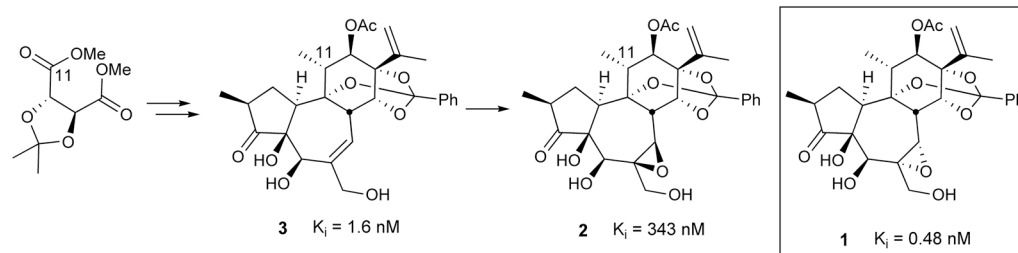


Figure 6.

**Figure 7.**

**Figure 8.**

**Table 1**Biological evaluation of **1**, **2**, and **3**.

	PKC affinity	cellular growth inhibition	
	K <sub>i</sub> (nM) <sup>a</sup>	A549 EC <sub>50</sub> (nM) <sup>b</sup>	K562 EC <sub>50</sub> (nM) <sup>b</sup>
<b>1</b> <sup>c</sup>	0.48 ± 0.07	150 ± 30	7 ± 1
<b>2</b>	343 ± 6	>10,000	>10,000
<b>3</b>	1.6 ± 0.1	1500 ± 60	87 ± 5

<sup>a</sup>K<sub>i</sub> values determined in duplicate experiments.<sup>b</sup>EC<sub>50</sub> values determined in triplicate experiments. All errors shown are standard errors of the mean.<sup>c</sup>A sample of yuanhuapin **1** was provided by Prof. Yue, Shanghai Institute of Materia Medica, Chinese Academy of Sciences, Shanghai, China.